Journal of Membrane Science and Research 5 (2019) 55-64

Journal of Membrane Science & Research

journal homepage: www.msrjournal.com

Research Paper

Fluorosilaned-TiO_2/PVDF Membrane Distillation with Improved Wetting Resistance for Water Recovery from High Solid Loading Wastewater

Nur Suhaili Mohd Yatim [1], Ooi Boon Seng [2,*], Khairiah Abd. Karim [2]

[1] *Faculty of Engineering Technology, Universiti Malaysia Perlis,Sungai Chuchuh, 02100 Padang Besar , Perlis, Malaysia*
[2] *School of Chemical Engineering, Engineering campus, Universiti Sains Malaysia, Seri Ampangan, 14300 NibongTebal, Penang, Malaysia*

Article info

Received 2018-07-02
Revised 2018-09-03
Accepted 2018-09-24
Available online 2018-09-24

Keywords

Membrane Distillation (MD)
Fluorosilane
Thermal Efficiency (TE)
Wetting
High solid loading wastewater

Highlights

- Silanization of TiO_2 at higher pH gave better particle distribution
- PVDF embedded with flurosilanized TiO_2 at higher pH produce hydrophobic membrane
- The hydrophobic membrane is fouling resistance towards oil-free high solid loading waste
- The hydrophobic membrane is susceptible for pore blocking for oily wastewater
- Fouling caused the drop of system thermal efficiency

Graphical abstract

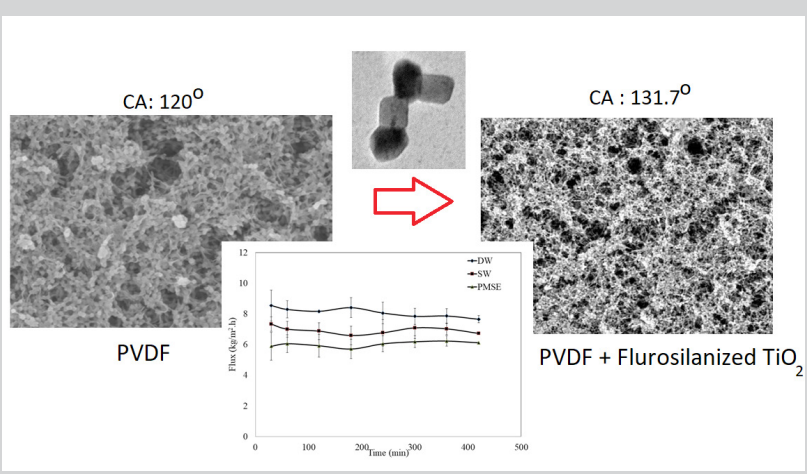

Abstract

Membrane distillation (MD) has emerged as an important technology for applications in industries such as seawater desalination and wastewater treatment due to its low energy requirement and theoretically low fouling propensity. However, the main obstacle to obtain high separating efficiency in MD lies on the availability of porous hydrophobic membrane that can withstand pore wetting and membrane fouling. In this work, a dual coagulation bath method was introduced to alter the membrane morphology by increasing its porosity, surface roughness as well as polymer crystallinity. To increase the membrane hydrophobicity, membrane roughness was induced by adding TiO_2 nanoparticles. However, this has brought concomitant impacts by lowering its porosity due to the pore blocking and reducing hydrophobicity due to the presence of hydroxyl group on TiO_2 surface. Introduction of silanized TiO_2 modified at pH 7 gave higher contact angle (131.7±4) that could withstand the pore wetting and at the same time maintained its high permeation flux (12kg/m².h) and excellent nutrient removal efficiency of 99.65%. Consistent flux around 6 kg/m².h for Paper Mill Sequence Batch Reactor (PMSE) could be achieved showing that the membrane wetting and fouling resistance towards solids were good. The system efficiency was around 55% which was comparable to the pure water treatment process (50%). However, the membrane was not suitable to be used for treatment of the oil-rich Palm Oil Mill Effluent (POME) as the flux dropped from 6 to 2 kg/m².h after 7 hours of operation with thermal efficiency dropped to 26% due to fouling phenomena.

1. Introduction

Membrane surface was commonly subjected to various modifications to acquire the surface with low surface energy for membrane distillation application. However, the modification process via chemical route is time consuming and costly. To solve this problem, membrane surface properties could be altered by changing its physico-chemical properties via hydrophobic nanoparticles incorporation. Various type of nanoparticles have been used for modification of organic membranes, such as SiO_2 [1], Al_2O_3 [2], Fe_3O_4 [3] and TiO_2 [4, 5] which aims to improve the performance and antifouling properties of the membranes. Among all, TiO_2 exhibited outstanding antifouling and antibacterial properties and it can be potentially used for membrane performance enhancement [6, 7]. Damodar and Rahimpour investigated the antibacterial properties of membrane that was entrapped with TiO_2. The TiO_2 modified nanocomposite membrane exhibited improved antibacterial properties with the aid of UV light due to photocatalytic property of TiO_2 [7]. However, the presence of TiO_2 could change the membrane surface from hydrophobic to hydrophilic due to the presence of hydroxyl group. Although, hydrophilic TiO_2 can improve the antifouling properties of the membrane, it rendered the membrane with unwanted higher surface energy and it was not

* Corresponding author at: Phone: +60 45996418; fax: +60 45996908
E-mail address: chobs@usm.my (B.S.Ooi)

DOI: 10.22079/JMSR.2018.89172.1202

suitable for MD. On the other hand, Razmjou et al. turn the nanocomposite membrane into superhydrophobic membrane by creating a hierarchical structure and enhanced roughness by incorporating TiO_2 nanoparticles on microporous PVDF membranes via a low temperature hydrothermal (LTH) process. The liquid entry pressure (LEPw) improved nearly 60% and the membrane turned to superhydrophobic with water contact angle reaching 166° [4].

The motivation of this research therefore is to address the above shortcomings. This work aims to improve the membrane hydrophobicity by changing the morphology of the surface via incorporation of silanized nanoparticle. The strategies included roughness enhancement via particle incorporation while maintaining the structural stability. Further hydrophobicity enhancement can be achieved via creating hierarchical surface roughness and made possible by modifying the TiO_2 and controlling their distribution on the membrane surface to enhance the co-continuous structure and membrane wettability. Applications of MD in various industries are being explored for different feed characteristic especially for high solid loading waste stream. Resultantly, the need for understanding fouling/wetting becomes more relevant under the circumstances of cake layer formation. In view of this, we extended this study to the real wastewater system which consists of high solid loading such as palm oil mill effluent and paper mill effluent which have never been reported.

2. Experimental

2.1. Materials

Porous flat sheet membranes were fabricated from polyvinylidene fluoride, PVDF (Solef® TA6010, Solvay Solexis). The casting solutions were prepared by dissolving predetermined PVDF in N-methyl-2-pyrrolidone, NMP (Merck, Germany) (purity (GC) ≥99.5%). Titanium Dioxide, TiO_2 Degussa P25 was used as membrane additive from Degussa. Trimethoxy (3,3,3-trifluoropropyl)silane purchased from Sigma Aldrich was used to modify the TiO_2.

2.2. Membrane preparation

2.2.1 Preparation of composite PVDF/TiO_2 membrane

Titanium dioxide (P25) was ground by using a mortar and pestle to reduce the number of large agglomerate. 0.1g TiO_2 was subjected to ultrasonic dispersion in 80 ml of NMP for 15 minutes. 20 % PVDF were then dissolved in the NMP/TiO_2 solution at 40ºC for 24 hours. The polymer solution was then cast on a flat glass plate wrapped with tightly woven polyester (style 0715 Dacron Fabric, Texlon Corporation, USA) with the thickness of 200 µm using automatic thin film applicator (Elcometer 4340). The nascent membrane was immediately transferred into isopropanol coagulation bath for 2 seconds and then immersed in water coagulation bath for 24 h to allow total solidification of the polymer with desired morphology (high porous and roughness) and to completely remove the residual solvent [8]. The membrane formed was removed from the water bath and further air-dried for 1–2 days [9].

2.2.2. Preparation of silanized-TiO_2-PVDF composite membrane under different modification conditions

The coating of fluorosilane was taken place via hydrolysis and condensation reactions. Firstly, 2.0 g of untreated TiO_2 nanoparticles were dispersed in 50 mL ethanol solution by ultrasonic agitation for 15 min. To hydrolyze the fluorosilane before coating on the TiO_2 nanoparticles, 1 ml of 1 M Trimethoxy(3,3,3-trifluoropropyl)silane solution (fluorosilane) was added to 20 mL ethanol at predetermined pH of 2, 7 and 12 and mixed for 1 h. The pH of TiO_2 suspension was also adjusted using 1 M HCl and 1 M of NaOH solution to the respective pH of 2, 7 and 12. Then, the hydrolyzed fluorosilane was gradually added to the TiO_2 suspension under the same pH and it was stirred in the dark condition for 24 h. Afterwards, the solid product was obtained by centrifugation at the rotational speed of 8000 rpm. The solid particles were re-suspended and recollected for another 3 times using pure ethanol. After that, the modified particles were dried in an oven at 105ºC for 2h. The silanized TiO_2 were labeled as T-Si-2, T-Si-7 and T-Si-12 for pH 2, 7 and 12, respectively. The silanized TiO_2 were then dispersed into the 20% of PVDF solution and denoted as MT-Si-2, MT-Si-7 and MT-Si-12 following the TiO_2 particles modified at pH of 2, 7 and 12, respectively.

2.3. Preparation of feed solutions

The feed solutions that were utilized in this work include distilled water, synthetic nutrient solution, PMSE and POME. Distilled water and synthetic water were used to characterize the membrane performance from the aspects of flux and retention capability. The membrane distillation system was subjected to two real wastewater filtration namely paper mill effluent represents solution with high suspended solid while the POME was to test on the solution that was rich in solid contents.

2.4. Distilled water

Distilled water was produced in the laboratory using single stage water distiller (ROSS R4000).

2.5. Synthetic nutrient solution

Synthetic nutrient solution was prepared as a testing solution to check on the retention performance of the membrane. If wetting occur, it was expected that the permeate COD will be increased. Nutrient solution was prepared by mixing 3.8 g/L glucose, 1.8 g/L peptone, 0.067 g/L sodium bicarbonate, 0.047 g/L magnesium sulphate, 0.24 g/L monopotassium phosphate, 0.3 6g/L dipotassium phosphate and 0.047 g/L calcium chloride in 1L of distilled water [10].

2.6. Palm oil mill effluent (POME)

Raw POME was sampled from a local Palm-Oil Mill industry, Perak. The sample was kept in cool room before testing and was used as it without further dilution. Oil and grease of POME were 294-452 mg/L and total solid were around 24,600 – 40,600 mg/L

2.7. Paper mill sequence batch reactor effluent (PMSE)

PMSE was taken from a local Paper Mill, Pulau Pinang. The sample was kept in cool room prior to the testing and was used as it without further dilution. The hardness ($CaCO_3$) and total dissolved solid of the PMSE were 306 mg/L and 404 mg/L, respectively.

2.8. Membrane and TiO_2 characterization

2.8.1. Surface and cross-sectional morphology checking

For morphology observation, the membranes were initially air dried. For cross-sectional morphology checking, the membranes were dipped in liquid nitrogen then cracked to obtain a brittle and clean fracture [11]. Firstly, the membrane samples were cut into suitable size before mounted onto the sample holders. Next, the membrane samples were coated with a conducting layer of gold to avoid charge accumulation on the membrane surface [12, 13]. The morphologies of the PVDF membranes were observed using SEM (Hitachi TM-3000 Table Top SEM).

2.8.2. Pore sizes and liquid entry pressure of membranes

The pore size of membranes was evaluated using Capillary Flow Porometer (Porolux 1000, Belgium). The membrane sample was cut into a 10cm circular coupon and then analyzed using the “dry up–wet up” technique. To calculate the average pore size, the cumulative pressure was used. This method measures only the smallest diameter of the capillary pore [11, 12]. The pore sizes were estimated using perfluoroether (porefil) solution whereas the water liquid entry pressure (LEPw) was evaluated using pure water and analyzed using PMI software [12].

2.8.3. Membrane wettability

The membrane wettability was evaluated via the static contact angle (CA) of the membrane samples. This was measured with a DropMeter A-100 contact angle system (Rame-Hart, U.S.A.) based on sessile drop method. The sample was taped flatly onto a glass slide with the membrane surface facing upwards. 13 µL of deionized water or distilled water was dropped with a microsyringe onto the dry sample surface. Then, a microscope was used to capture the micrographs. This microscope setup has long working distance 6.5×objectives with high frequency (100 Pcs/s). The contact angles were measured from 10 different spots of membrane sample and then averaged to reduce the random error.

2.8.4. Surface roughness

Atomic Force Microscopy or AFM (Model XE 100, Park System) was used to analyze the membrane surface roughness and topography via noncontact mode. The membrane samples with the dimension of 0.5 cm × 0.5 cm were fixed on a magnetic holder with carbon tape. All AFM images were observed under room temperature. Scan areas (12.5 × 12.5 µm) were randomly selected and the roughness parameters, the average of a set of individual measurements of a surfaces peaks and valley (R_a) were determined [8].

2.8.5. Thermal conductivity

The effective conductivity of the membrane, k_m, can be measured using the thermal constants analyzer (hot-disk TPS 2500 S) which applies the Transient Plane Source (TPS) technique [15]. For this measurement, a membrane was cut into the size of 5cm x 5cm. The sensor with radius 6.403 mm was chosen and the results were averaged from 5 measurements [16].

2.8.6. Particle shape and size analysis

Transmission electron microscopy (TEM) (JEOL, JEM-20CX) was employed to determine the primary core size and shape of the particle. The TiO_2 samples were immersed in alcohol solution for 15 minutes before observed under TEM. A single droplet of particle suspension (low concentration to avoid particle overlapping) was placed onto a TEM grid holder and left to air dried in room temperature for several minutes. The sample specimen was then viewed using TEM under different magnification. The entire sample was observed under 200 kV.

2.9. Study on the Antibacterial properties of membranes

2.9.1. Bacteria inoculation

Bacillus Subtilis and *E.coli* obtained from the Industrial Biotechnology Research Laboratory (Malaysia) were used in the antibacterial test. The bacteria were stored in freezer at -18ºC before use and kept in the refrigerator at 3 ºC prior to inoculation. The bacteria were anaerobically grown in a sealed flask consists of nutrient broth. The medium was first sterilized in an autoclave at temperature of 121 °C and pressure of 15 psig for 20 min. The medium pH was adjusted to 7.1. The inoculums were introduced into the medium at ambient temperature. *Bacillus Subtilis* was incubated at 25-35 °C for the duration of 48 h [7, 17] while *Escherichia coli, (E. Coli*) was incubated at 37 °C for the duration of 48 h [18].

2.9.2. Membrane biofouling testing

The membranes were cut into small pieces (1 cm x 1cm) and rinsed with phosphate buffer saline (PBS) solution before immersing in the sterilized deionized water for 24 hours. Then the membranes were immersed in the inoculated culture for 48 hours. The extent of bacteria growth on the membrane surface was served as an indicator for the bio-fouling phenomenon. After 48 hours, the membrane with *Bacillus Subtilis* was rinsed with phosphate buffer saline (PBS) solution, 3% glutaraldehyde and dehydrated with serial of ethanol solutions while for *E.coli*, the membrane was rinsed with phosphate buffer saline (PBS) solution and 3% glutaraldehyde without using ethanol solution to prevent the total wash out of *E.Coli* from the surface due to its unattached nature. The membrane was then observed under SEM at 5 kV [18]. This method was compared with bicinchoninic acid assay (BCA) Kits which is a biochemical assay that determine the total concentration of protein produced by the bacteria. To prepare this kit, 2 ml BCA solution was mixed with 40 µL cupric sulfate. This solution was dropped on the membrane surface and left for 35 minutes. The original green colour of the solution will change to purple if the surface contains protein/ bacteria.

2.10. Membrane Performance Test

2.10.1. Permeation flux and Chemical Oxygen Demand (COD) retention study

A laboratory scale direct contact membrane distillation (DCMD) unit (see Figure 1) was utilized to study the membrane permeation flux and solute retention using distilled water and synthetic nutrient solution as model solutions. The porous membranes with different morphology were tightly clamped between two acrylic plates to separate the hot and cold flow streams. The effective area of the membrane being used in this experiment was 16 cm x 6 cm while the channel depth on each side is 1.5 cm. The feed solution was heated to the desired temperature by placing it in a hot water bath (Protech HC-10). The hot stream flew below the porous membrane while the cold stream was on top of it. The donor cell (hot stream) was circulated in the donor cell under the different temperature of 50°C, 60°C, 70°C, 80°C and 90°C. While in the cool site, the chiller temperature was kept constant at 16ºC. The distillate was continuously recirculated within the permeate loop and was cooled to the desired permeate temperature using a chiller (Huber mini chiller) with mixed water/glycerol as the refrigerant. The flow rate was regulated by a speed variable peristaltic pump (Masterflex L/S Cole-Parmer) at atmospheric pressure. The flow rate of the cold and hot feed for this experiment were maintained at 300 cc/min and 100 cc/min, respectively[19]. Concentrations (COD) of the solution in both feed and permeate streams were determine using Lovibond®maxidirect portable photometer [20].

The permeate reservoir was a 1 L jacketed flask that allows the overflow of excess water which results from vapor permeation process. The overflow from the reservoir because of water being transferred from feed to permeate side was collected and continuously weighted on an electronic balance (A&D company limited FX-3000i). The data at 60 s interval was directly transmitted to computer via data-logger. At the end of the experiment, samples were collected from the permeate reservoir for COD checking. The membrane flux was calculated based on the mass of condensate collected in the permeate chamber within a predetermined duration over the effective area.

The permeation flux of the membranes *J* is determined using Eq. (2):

$$J = \frac{\Delta W}{A \Delta t} \quad (1)$$

where J is the permeation flux ($kgm^{-2}h^{-1}$), ΔW is the quantity of distillate (kg), A is the effective inner surface area of the porous membranes (m^2) and Δt is the sampling time (h) [21, 22].

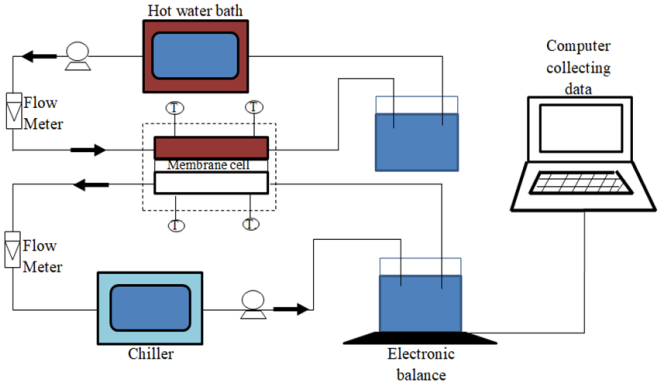

Fig. 1. The schematic diagram of direct contact membrane distillation setup.

Rejection of synthetic nutrient water, $R_{\text{synthetic water}}$ was determined using equation below:

$$R_{synthetic\ water} = \left(1 - \frac{M_{tank}\left(1 + \frac{V_{tank} \times 1000}{J_w A_m t}\right)}{C_F}\right) \times 100 \quad (2)$$

where V_{tank} is the volume of permeate reservoir (m^3), M_{tank} is the COD in the permeate solution tank, C_F is the initial COD in the feed, A_m is the membrane area (m^2), and *t* is time (h).

2.10.2. Chemical Oxygen Demand (COD) Test

The COD of the permeate was measured based on the standard method from Lovibond®maxidirect portable photometer. For the preparation of the blank sample, 2 ml of distilled water were added into the Lovibond COD reagent vial by using micro pipette. For COD sample preparation, 2 ml of filtered water sample were added into the new reagent vial and both vials were heated up for 120 minutes at 150°C by using Thermo-reactor. The vials from the heating block were then removed and allowed to cool down until temperature around 60°C or less. Each vial was then inverted several times while still warm to mix the contents and allowed to cool to ambient temperature before measuring the COD value by using Lovibond® kit.

2.10.3 Performance evaluation of the direct contact membrane distillation process

In this experiment, the feed solution was synthetic water, POME, and PMSE. The donor cell (hot stream) was circulated in the donor cell under different temperature while the permeate temperature was maintained around 16ºC. The system was run for 2 to 8 hours whereby the concentrations of the solution in both feed and permeate stream will be determined periodically using COD reagent. Flux profile was continuously monitored using the electronic balance (A&D company limited FX-3000i) and the data was directly transmitted to computer at 1 min interval.

2.10.4. Temperature polarization coefficient (TPC) determination

Temperature polarization coefficient (TPC) is the function of both feed and permeates boundary layers' temperature. It depends on the

hydrodynamics behaviors, fluid properties and operating conditions. It is defined as the ratio of actual driving force to the overall driving force as below [23]:

$$\text{TPC}=\frac{T_{fm}-T_{pm}}{T_f-T_p} \tag{3}$$

where T_f and T_p are the bulk feed and permeate temperatures. T_{fm} and T_{pm} are the temperatures of the liquid/vapor interface at the membrane surface pores of the feed and permeate sides, respectively.

The correlation between mass and heat transfer across the membrane from the feed to the permeate must be determined to calculate the TPC. The heat transmitted through the feed and permeate boundary layers is defined by Eq. (5-6) respectively while the heat transferred through the membrane is defined by Eq. (7) [23].

$$\dot{Q}_f=h_f A(T_f-T_{m,1}) \tag{4}$$

$$\dot{Q}_p=h_p A(T_{m,2}-T_p) \tag{5}$$

$$\dot{Q}_m=A\left(N\Delta H_{LV}+\frac{k_m}{\delta}(T_{m,1}-T_{m,2})\right) \tag{6}$$

where Q is the heat transfer rate (W), h refers to the heat transfer coefficient (W/m^2 K), A is the membrane area (m^2), N is the permeate flux (kg/m^2 s),ΔH_{LV} is the latent heat of vaporization (J/kg), k_m is the effective membrane conductivity (W/m.K) and δ is the nominal membrane thickness (m). Subscripts f and p represent feed and permeate, respectively. $m,_1$ *and* $m,_2$ represent the temperature at the membrane boundary layer of the hot side and cold side, respectively. The effective conductivity, k_m, can be estimated from thermal conductivities equipment, thermal constants analyzer (hot-disk) [15].

Under steady-state conditions, the membrane surface temperatures can be defined as follows [20]:

$$\dot{Q}_f=\dot{Q}_m=\dot{Q}_p \tag{7}$$

$\dot{Q}_f$ is the heat transfer rate (W) for feed side, $\dot{Q}_m$ is the heat transfer rate (W) across the membrane, and $\dot{Q}_p$ is the heat transfer rate (W) for permeate side.

$$T_{m,1}=\frac{\frac{k_m}{\delta}\left(T_p+\left(\frac{h_f}{h_p}\right)T_f\right)h_f T_f-N\Delta H_{LV}}{\frac{k_m}{\delta}+h_f+\frac{k_m}{\delta}.\frac{h_f}{h_p}} \tag{8}$$

$$T_{m,2}=\frac{\frac{k_m}{\delta}\left(T_f+\left(\frac{h_p}{h_f}\right)T_p\right)h_p T_p-N\Delta H_{LV}}{\frac{k_m}{\delta}+h_p+\frac{k_m}{\delta}.\frac{h_p}{h_f}} \tag{9}$$

The heat transfers coefficients of the feed and permeate boundary layers are expressed as

$$h_f=\frac{Nu_f k_f}{d_h},\quad h_p=\frac{Nu_p k_p}{d_h} \tag{10}$$

where the Nusselt numbers, Nu, and thermal conductivity, k_f *and* k_p, are the local feed and permeate fluid properties respectively. Nusselt number in this case was assumed to be calculated based on turbulent flow whereby equation (12) is valid for moderate temperature differences ΔT and the following Nusselt number correlation from Dittus Boelter were applied to calculate the mass transfer coefficient.

$$Nu=0.023Re^{0.8}Pr^n \tag{11}$$

when n=0.4 for heating; n=0.3 for cooling, Re is Reynold number and Pr is Prandtl number.

2.10.5. Thermal efficiency (TE)

Thermal efficiency (TE) is defined as the ratio of the heat transferred with the vapors to the total heat transmitted across the membrane [20].

$$TE\ (\%)=\frac{JH_v\{T\}}{JH_v\{T\}+(K_m/\delta)(T_{fm}-T_{pm})}\times 100 \tag{12}$$

where K_m is the thermal conductivity of membrane as in equation (7) (W/m.K), δ is membrane thickness (m), T_{fm} and T_{pm} are the temperatures of the liquid/vapor interface at the membrane surface pores (K), J is the flux (L m^{-2} h^{-1}), ΔW is the quantity of distillate (L), A is the inner surface area of the porous membranes (m^2), Δt is the sampling time (h) and H_v is the enthalpy of vapor. H_v is determined with the thermodynamic relationship at any temperature T as in equation (13)

$$H_v(T)=1.7535T+2024.3 \tag{13}$$

3. Results and discussion

3.1. Morphology of silane treated TiO_2 nanoparticles

The images of TiO_2 treated with trimethoxy(3,3,3-trifluoropropyl)silane at different pH were observed under TEM. Nanoparticles were dispersed in the ethanol solution for 15 mins before observing the images. From Figure 2, it was found that the original TiO_2 (without treatment) or UT had significant agglomeration phenomenon compared to the fluorosilane-treated TiO_2. The same observation was found by other researchers [4] who found that chemical modification of nanoparticle with silane was able to reduce the agglomeration of nanoparticle. Figure 2 shows that pH 7 (T-Si-7) and pH 12 (T-Si-12) were the best conditions for fluorosilane treatment as it showed less agglomeration compared to pH 2. These observations were in accordance to the findings by [24] who found that appropriate flurosilane treatment could be achieved in neutral and alkali conditions whereby both hydrolysis and condensation reactions occur simultaneously. Coating a highly non-polar material like trimethoxy(3,3,3-trifluoropropyl)silane onto a polar TiO_2 could be achieved by tuning the surface of the TiO_2 become less polar or at isoelectric point. Studies by Su et al indicated that isoelectric point of TiO_2 powder was within pH 5-6.8 [25]. This explains why surface silanization was also efficient at pH 7 whereby the hydrolysis can be induced by the water itself.

3.2. Chemical properties of silane-treated TiO_2

Figure 3 shows the FTIR spectra of pristine TiO_2 nanoparticle before and after fluorosilane treatment. TiO_2 has characteristic peaks detected at 1628 and 3202 cm^{-1} [24] attributed to -Ti-O-Ti- group [26] whereas the C-F peak of T-Si-7 and T-Si-12 at 1400 cm^{-1} had higher intensity compared to T-Si-2 which means that the fluorosilane (with – CF_3) was coated well on TiO_2 nanoparticle at neutral and alkaline conditions.

3.3. Pore size and Wettability analysis of Silane/TiO_2 nanocomposite membrane

Figure 4 shows that after treating the TiO_2 with silane, the composite membrane gave mix response towards the surface wettability. However, the value of contact angle and LEPw were increased after treating the TiO_2 with silane under pH 7. This is in accordance to the FTIR results obtained in Figure 3 in which the surface silanization (coverage) was high at pH 7 and at the same time, the surface was less polar due to its pH that closed to isoelectric point. The surface coated with flurosilane was more hydrophobic compared to the pristine TiO_2 and therefore the contact angle increased from 116.24^0 to 131.7^0. Although T-S-12 has similar dispersibility likes T-S-7, the tendency of the TiO_2 surface to acquire negative charge at high solution pH had increased the membrane polarity which resulted in lower contact angle. In overall, the LEPw was lower than 1 bar mainly due to the bigger pore size on the membrane surface. The coating has proven to be effective in creating the hydrophobic surfce but liquid entry pressure depends on pore size, pore structure as well as surface hydrophobicity. In this case, the enlarged pore size was obtained as a result of dual coagulation bath method which resulted in low LEPw.

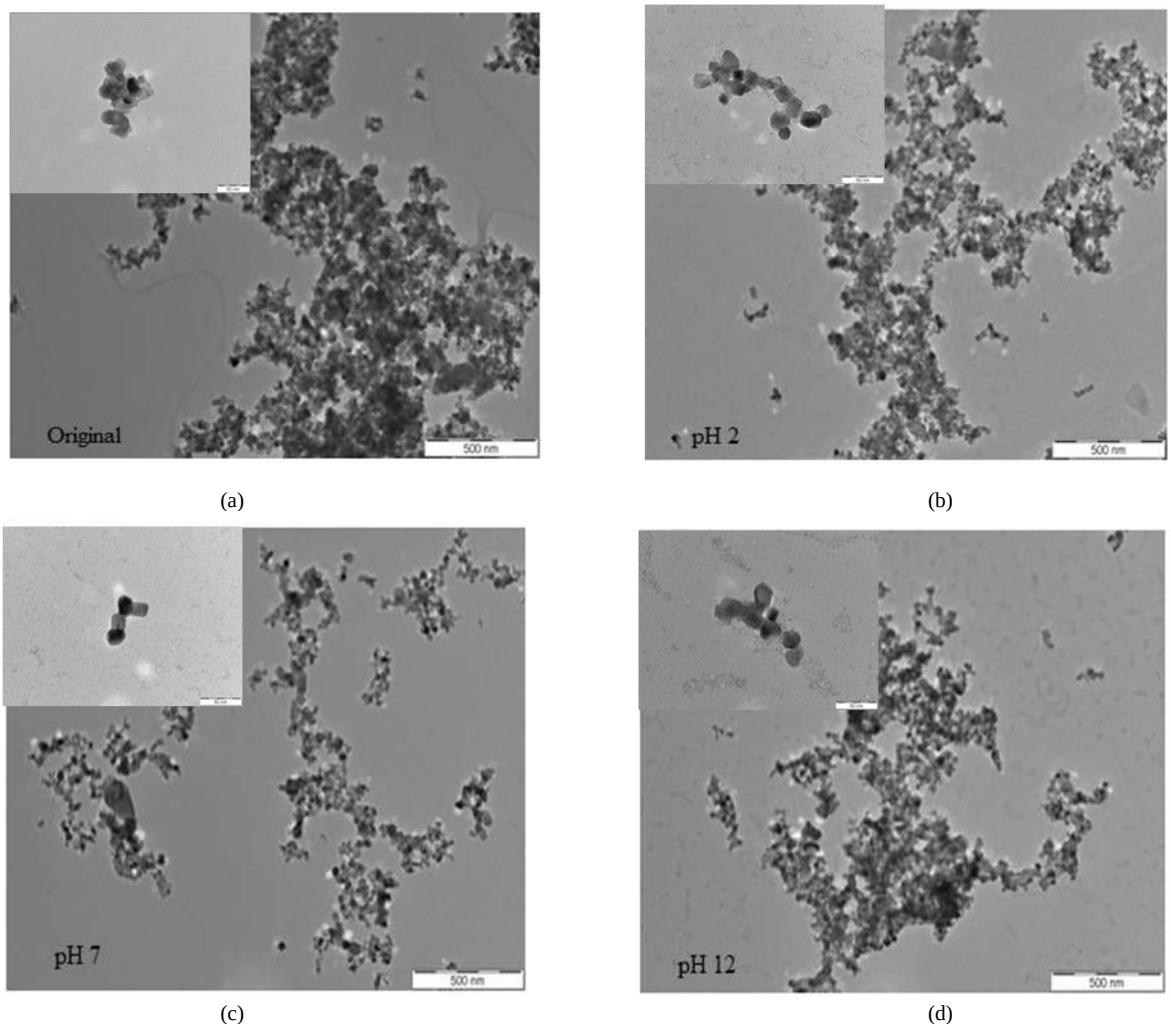

Fig. 2. TEM images of TiO_2 silanized at (a) Untreated (UT), (b) pH 2 (T-Si-2), (c) pH 7 (T-Si-7) (d) pH 12 (T-Si-12).

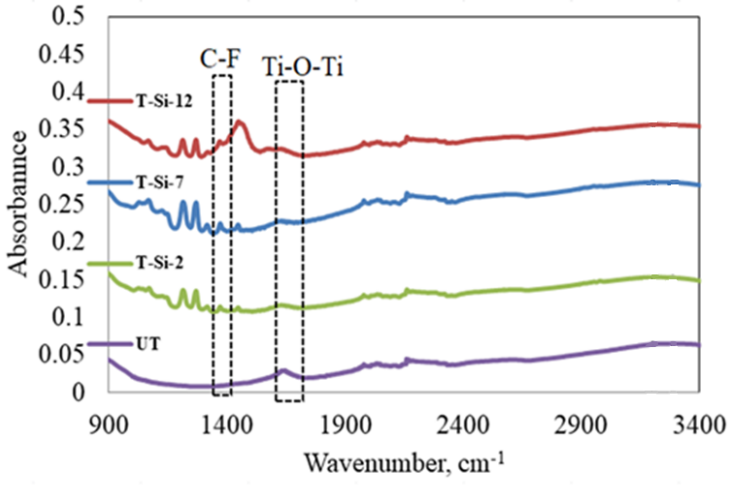

Fig. 3. FTIR spectra of untreated TiO_2 (UT) and silane-treated TiO_2 under different pH (T-Si-2, T-Si-7 and T-Si-12).

As shown in Figure 5, the surface roughness of membrane increased after treating the TiO_2 with fluorosilane at pH 7 and pH 12. The acidic TiO_2 which has net positive charge gave higher compatibility with the negatively charged PVDF matrix which improved the dispersion of T-Si-2; therefore, its roughness was the lowest. Rougher membrane surface was obtained for the negatively charged particle due to the repulsion effect. This gave membrane with higher contact angle which can be reflected by MT-Si-7 membranes.

3.4. Surface morphology of the silane treated TiO_2 nanocomposite membrane

Figure 6 shows that the bi-continuous structure of membrane was maintained even after silane modification. However, significant changes on the membrane morphology were observed for their surface pore size and porosity. After treating the TiO_2 with silane at pH 2, the pore size of the membrane was decreased. However, membrane with silane/TiO_2 at pH 7 and

pH 2 showed significant increment of surface pore size and porosity. As discussed earlier, positively charged TiO_2 has better compatibility with the negatively charged PVDF matrix which produced smaller particle size that gave less microgap. On the other hand, the particle which modified under alkaline of neutral pH had relatively positive charge that could be repelled by the PVDF matrix which induced higher membrane porosity.

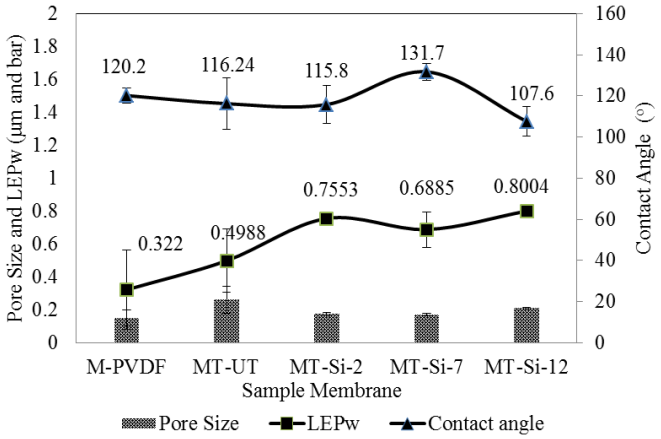

Fig. 4. Pore size, LEPw and contact angle of different membrane.

3.5. Antibacterial property on the silane treated TiO_2/PVDF membrane

The composite membranes were further tested for its antibacterial properties. Figure 7 shows that the pristine PVDF membrane (MT-0) and the membrane with untreated TiO_2 were seriously fouled by both B.*Subtilis* and *E.Coli* bacteria. It was noticed that all the silane treated TiO_2-PVDF membranes showed good antibacterial properties with limited growth of *E. Coli* on the membrane surface. On the other hand, amongst the silane treated TiO_2 membrane, only MT-Si-12 showed promising antibacterial properties towards B.*Subtilis*. Since the membranes were not exposed to the UV light, the antibacterial properties of the membrane were likely due to the failure of the bacteria adhere to the membrane surface due to its lower surface energy. This is especially true for the not attaching *E.Coli* whereby it was hardly detected on the membrane surface for all the silanized TiO_2 membrane. BCA kits showed that the green color for the silane treated TiO_2/PVDF membrane was not changed which indicated that no protein was being found on the surface.

3.6. Wettability study of silane/TiO_2 composite membrane

Based on the above membrane characteristic, membrane with flurosilane treated TiO_2 at pH7 (MT-Si-7) was chosen for further study due to its low wettability (higher contact angle) and anti-fouling properties that make it a suitable candidate for membrane distillation. Figure 8 shows that the membrane has stable flux over 400 min of operation for both distilled (DW) and nutrient rich water (SW). The stable flux of the membrane indicated that the membrane was not susceptible to wetting phenomena as pore wetting will lower the vapor permeation. The flux of the distilled water was slightly higher than the flux of nutrient water due to the concentration polarization effect. The concentrating effect of the nutrient near the surface of the membrane lowered down the vapor pressure of water at the interface. Therefore, its thermal driving force across the membrane was reduced.

3.7 Performance of MT-Si-7 on the real wastewater filtration

The membranes were challenged with two types of industrial effluent namely PMSE and POME. The reason of choosing these effluents was because both wastewaters have high load of suspended solid which was detrimental for membrane operation. The paper mill effluent has low COD value, but it contains a lot of algae and suspended solid ($CaCO_3$). As membrane distillation is proven to be able to resist fouling due to suspended solid, PMSE was chosen as the model solution. The membrane was also subjected to POME which has high solid content as well as high oil content.

Figure 9 shows the membrane flux profile for PMSE and its comparison to distilled water and synthetic water. It is clearly seen that the overall flux of the PMSE was lower than the distilled water and synthetic nutrient water. It was an expected trend due to the deposition of the cake layer on the membrane surface by the suspended solid (180 mg/l $CaCO_3$) as well as microalgae. However, it was important to note that the rejection of the system was maintained at 99% which shows that the membrane wettability phenomenon can be tolerated. Besides, the stable permeation flux also indicated that pore blocking was unlikely to occur even though the pores of membrane were up to 0.2 um.

Figure 10 shows that the cake layer forms immediately on the membrane surface upon filtering the PMSE. However, it was very important to note that, although the membrane has lower flux, it has consistent flux over 400 min of operation. This observation indicated that the membrane not only has superior wetting resistance but also has pore blocking resistance as could be proven by the membrane cross sectional image which showed no observable pore blocking phenomenon. The fouling was only occurred on the surface with loose cake layer due to the absence of pressure force. The cake layer exerts flow resistance for the conventional pressure driven process, but for such thermal driven process, the high solid content near the membrane surface caused reduction in the free water that lowering down its effective vapor pressure on the surface. The marginal decrease of flux showed that the cake layer should be porous enough to allow remarkable high-water permeation. The cake layer was relatively low density with the absent of pushing force as compared to the denser cake layer for the pressure driven process such as microfiltration and ultrafiltration.

MT-S-7 was further used to filter the POME. Compare to PMSE, the membrane performance was not promising for separating the oily wastewater like POME. The DCMD process was run for 7 hours to investigate its fouling characteristic using POME as feed solution. Based on Figure 11, it was found that the membrane flux was decreased drastically from 6 to 2 $kg/m^2.h$ over 400 min of operation, while maintaining the COD rejection of 96.9%±2.0. The same phenomenon was observed by others researcher in the pressure driven process in which membrane flux was declined with time during POME treatment. In view of this, wetting or fouling is most likely to occur that facilitates the permeation of organic compounds through the membrane.

As commonly known, POME has both high solid and oil content. For the POME treatment, the flux declination is certainly due to the pore blocking because of higher oil-membrane affinity. This can be clearly seen in Figure 12 that the membrane was badly fouled on the surface as well as on the porous substructure. The blockage was the main reason for the continuous flux declination of the membrane. The hydrophobic nature of oil can easily adhere to the porous surface of the membrane and cause serious fouling. Once the capillary force of the pore mouth was overcome, the fine oil emulsion could be easily transported through the pore via viscous flow and trapped within the torturous pore structure.

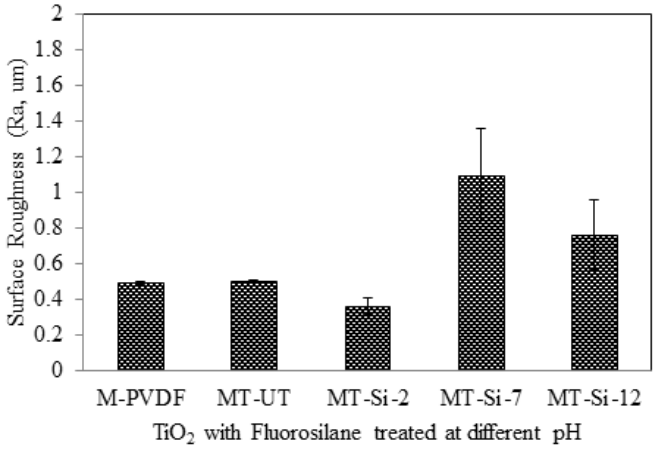

Fig. 5. Surface roughness (Ra, µm) of different membrane with TiO_2 modified at different pH.

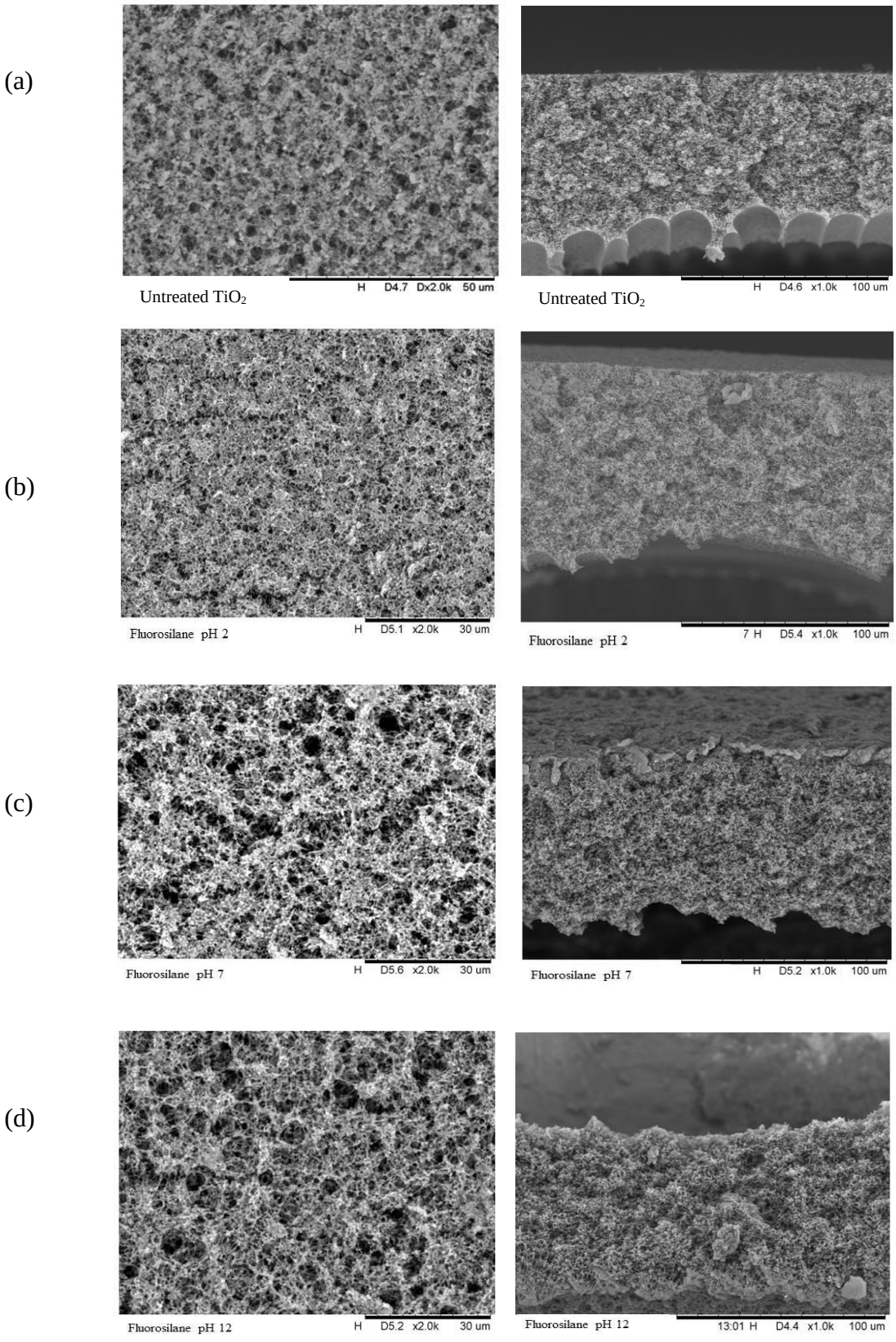

Fig. 6. Surface and cross section images of (a) MT-UT, (b) MT-Si-2 (c) MT- Si-7 and (d) MT-Si-12.

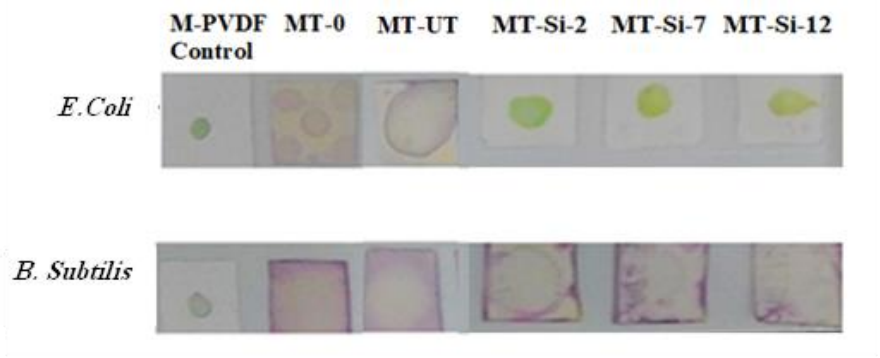

Fig. 7. BCA kits image bacteria *E.Coli* and *B.Subtilis* of M-PVDF, MT-UT, MT- Si-2, MT-Si-7, and MT-Si-12.

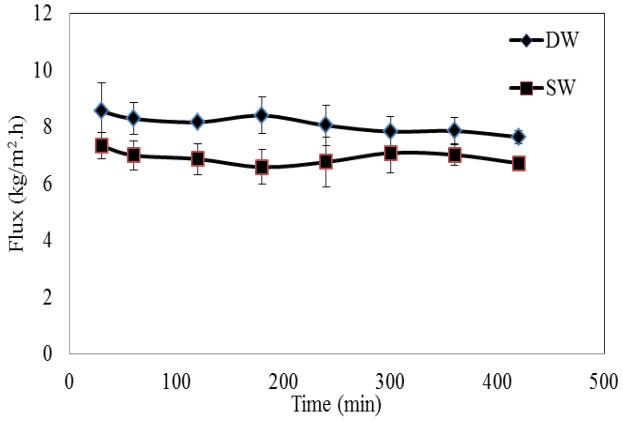

Fig. 8. Flux profile of MT-Si-7 tested based on distilled and nutrient rich water.

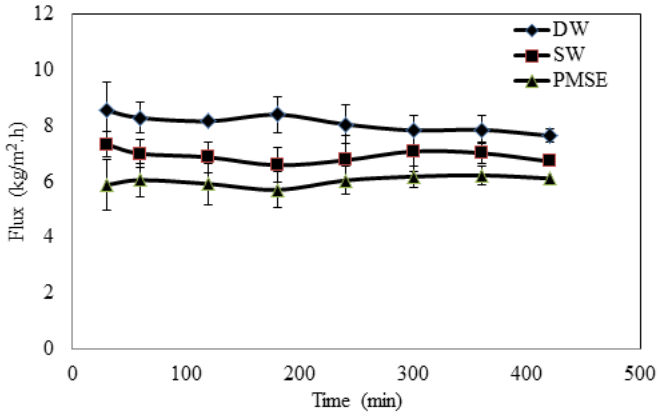

Fig. 9. Flux profile of MT-Si-7 for treating the PMSE.

(a)

(b)

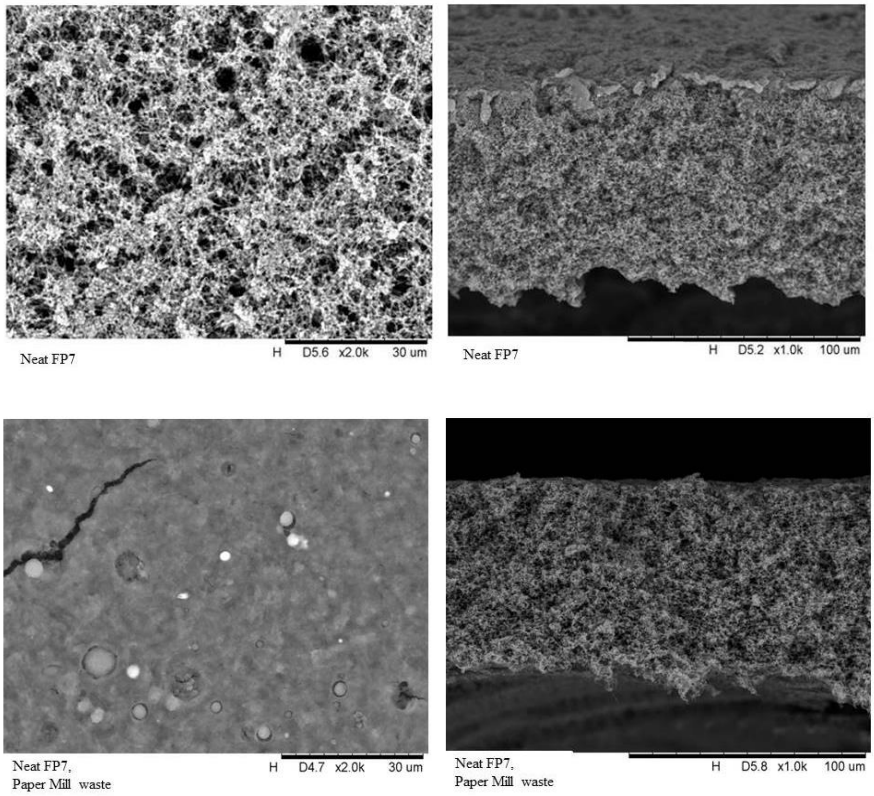

Fig. 10. Surface and cross-sectional SEM images of MT-Si-7 (a) before and (b) after treating the PMSE.

3.8. Thermal efficiency and temperature polarization concentration of membrane

Figure 13 shows that the thermal efficiency was decreased after running the POME and PMSE effluent. The dropped in system efficiency was due to the unavoidable wetting phenomenon as well as fouling problem. Thermal efficiency analysis provides a direct indication on the membrane wetting/fouling phenomenon. The pore wetting phenomenon brings along the heat loss due to the conduction through the medium-filled pores in addition to the lower convective transport of vapor due to surface and pore blocking. Both effects resulted in lower membrane thermal efficiency. In this case, the lowest thermal efficient of the POME system (28%) indicated that pores had been filled up with the oil which increased the heat loss via conduction and decreased vapor permeation due to pore blocking.

On the other hand, the thermal polarization effect was not significantly affected by the type of feed solution. Its values were maintained at the value of 0.7. The TPC is mainly controlled by the mass and heat transfer across the membrane. The solution viscosity seems to have insignificant effect on the hydrodynamic conditions at the boundary layer for both feed and permeate side. This finding is an indication that the cake layer was indeed porous enough that water vapor can be easily permeate the cake layer without creating a serious temperature polarization effect.

4. Conclusions

In this work, TiO_2 nanoparticles was modified by trimethoxy (3,3,3-trifluoropropyl)silane and dispersed within PVDF matrix to reduce the surface energy of the membrane. Membrane loaded with flurosilane modified at pH 7 shows the desired properties for membrane distillation with the highest contact angle (131.7°) that suitable to be applied in membrane distillation. Besides, the modified membrane has also good anti-biofouling properties especially towards the E.Coli. The optimum membrane showed that flux declination was negligible for a process involving high solid content like PMSE over a continuous operation of 7 hours because of low wetting and negligible pore blocking effect. However, the membranes showed poor wetting phenomenon towards palm oil mill effluent with significant pores blocking being observed with relatively poor thermal efficiency. Nonetheless, the cake layer formed on the membrane surface was porous enough that temperature polarization effect was not significant.

Acknowledgement

The authors gratefully acknowledge the financial support from Universiti Sains Malaysia (USM) Research University Grant (1001/PJKIMIA/8014012) and University Malaysia Perlis (SLAI 2013) for financial supports throughout the study.

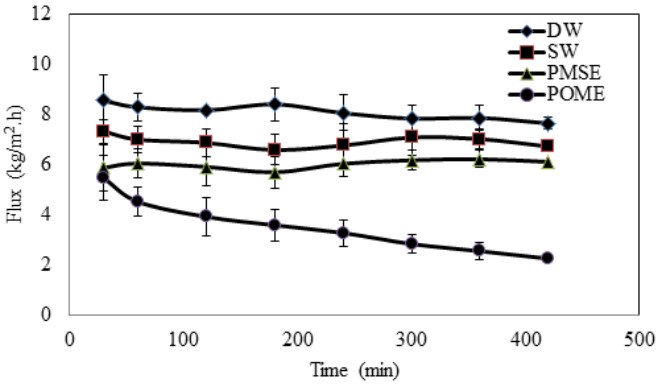

Fig. 11. Graph of flux (kg/m^2.h) versus time (min).

(a)

(b)

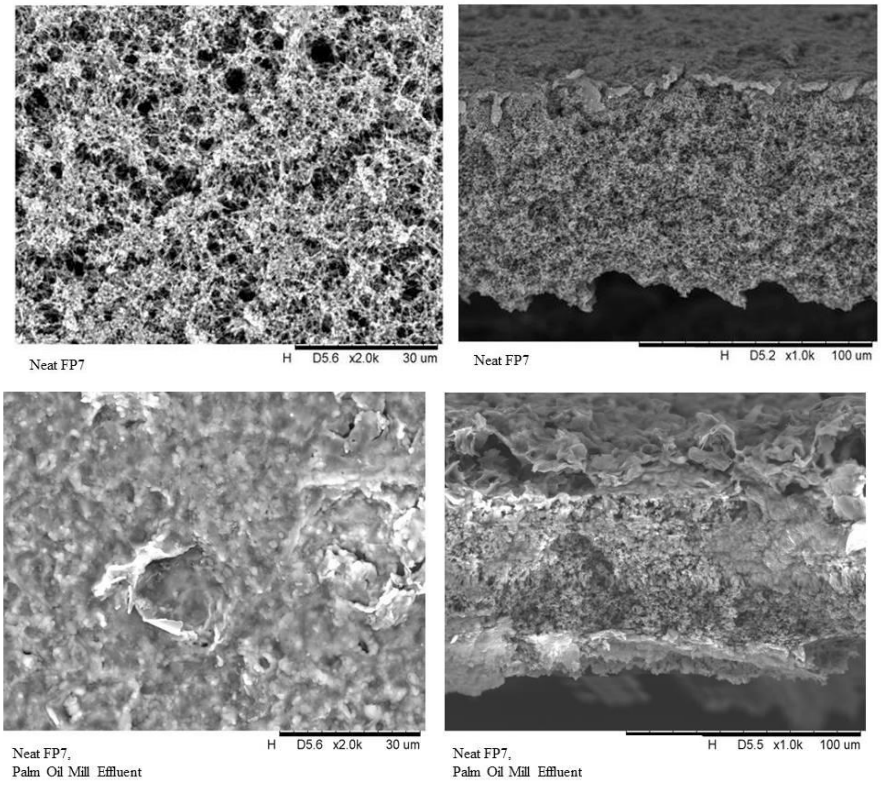

Fig. 12. SEM Images of the membrane (a) before and (b) after POME treatment.

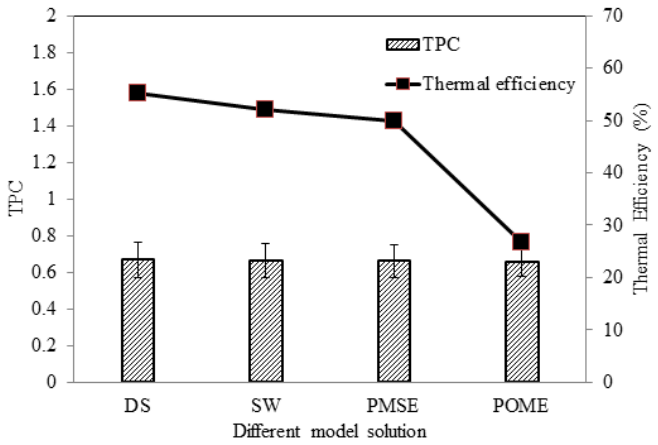

Fig. 13. TPC and thermal efficiency of membrane MT-Si-7 with different model solution.

References

[1] J. Zhao, M. Milanova, MMCG. Warmoeskerken, V. Dutschk, Surface modification of TiO_2 nanoparticles with silane coupling agents, Colloid. Surfaces A Physicochem. Eng. Asp. 413 (2012) 273–279.

[2] L. Yan, YS. Li, CB. Xiang, S. Xianda, Effect of nano-sized Al_2O_3-particle addition on PVDF ultrafiltration membrane performance, J. Membr. Sci. 276 (2006) 162–167.

[3] J. Du, L. Wu, C.Y. Tao, C.X. Sun, Preparation and characterization of Fe_3O_4/PVDF magnetic composite membrane, Acta Phys- Chim. Sin. 20 (2004) 598–601.

[4] A. Razmjou, A. Resosudarmo, R.L. Holmes, H. Li, J. Mansouri, V. Chen, The effect of modified TiO_2 nanoparticles on the polyethersulfone ultrafiltration hollow fiber membranes, Desalination 287 (2012) 271–280.

[5] X. Zhang, Y. Wang, Y. You, H. Meng, J. Zhang, X. Xu, Preparation, performance and adsorption activity of TiO_2 nanoparticles entrapped PVDF hybrid membranes, Appl. Surf. Sci. 263 (2012) 660–665.

[6] R. Damodar, S.-J. You, H.-H. Chou, Study the self cleaning, antibacterial and photocatalytic properties of TiO_2 entrapped PVDF membranes, J. Hazard. Mater. 172 (2009) 1321–1328.

[7] A. Rahimpour, M. Jahanshahi, B. Rajaeian, M. Rahimnejad, TiO_2 entrapped nano-composite PVDF/SPES membranes: Preparation, characterization, antifouling and antibacterial properties, Desalination 278 (2011) 343–353.

[8] B.S. Ooi, N.S.M. Yatim, A.L. Ahmad, S.O. Lai, Preparation of polyvinylidene fluoride membrane via dual coagulation bath system and its wettability study, J. Appl. Polym. Sci. 113 (2011) E225–E232.

[9] C.-Y. Kuo, H.-N. Lin, H.-A. Tsai, D.-M. Wang, J.-Y. Lai, Fabrication of a high hydrophobic PVDF membrane via nonsolvent induced phase separation, Desalination 233 (2008) 40–47.

[10] J. Phattaranawik, A.G. Fane, A.C.S. Pasquier, W. Bing, A novel membrane bioreactor based on membrane distillation, Desalination 223 (2008) 386–395.

[11] H.P. Ngang, B.S. Ooi, A.L. Ahmad, S.O. Lai, Preparation of PVDF–TiO_2 mixed-matrix membrane and its evaluation on dye adsorption and UV-cleaning properties, Chem. Eng. J. 197 (2012) 359–367.

[12] A.L. Ahmad, N. Ideris, B.S. Ooi, S.C. Low, A. Ismail, Morphology and polymorph study of a polyvinylidene fluoride (PVDF) membrane for protein binding: Effect of the dissolving temperature, Desalination 278 (2011) 318–324.

[13] Y.H. Teow, A.L. Ahmad, J.K. Lim, B.S. Ooi, Preparation and characterization of PVDF/TiO_2 mixed matrix membrane via in situ colloidal precipitation method, Desalination 295(2012) 61–69.

[14] A.L. Ahmad, W.K.W. Ramli, Hydrophobic PVDF membrane via two-stage soft coagulation bath system for membrane gas absorption of CO_2, Sep. Purif. Technol. 103 (2013) 230–240.

[15] V. Bohac, M.K. Gustavsson, L. Kubicar, S.E. Gustafsson, Parameter estimations for measurements of thermal transport properties with the hot disk thermal constants analyzer, Rev. Sci. Instrum. 71 (2000) 2452–2455.

[16] C. Time, T. Conductivity, Measurements on highly conductive alloys (copper and copper + zink alloy) and commercial PMMA, Hot Disk AB (2004) 5–6.

[17] V. Scuderi, M.A. Buccheri, G. Impellizzeri, A.D. Mauro, G. Rappazzo, K. Bergum, B.G. Svensson, V. Privitera, Photocatalytic and antibacterial properties of titanium dioxide flat film, Mater. Sci. Semicond. Process 42 (2016) 32–35.

[18] X. Li, T. Cai, T.-S. Chung, Anti-fouling behavior of hyperbranched polyglycerol-grafted poly(ether sulfone) hollow fiber membranes for osmotic power generation, Environ. Sci. Technol. 48 (2014) 9898–9907.

[19] N.S.M. Yatim, K.A. Karim, O.B. Seng, Performance of chemically modified TiO_2-poly (vinylidene fluoride) DCMD for nutrient isolation and its antifouling properties, J. Membr. Sci. Res. 2 (2016) 163–168.

[20] A. Ali, F. Macedonio, E. Drioli, S. Aljlil, O.A. Alharbi, Experimental and theoretical evaluation of temperature polarization phenomenon in direct contact membrane distillation, Chem. Eng. Res. Des. 91 (2013) 1966–1977.

[21] M. Khayet, C. Cojocaru, M.C. García-Payo, Experimental design and optimization of asymmetric flat-sheet membranes prepared for direct contact membrane distillation, J. Membr. Sci. 351 (2010) 234–245.

[22] M. Khayet, Membrane distillation: Principles and applications, Elsevier, 2011.

[23] Ó. Andrjesdóttir, C.L .Ong, M. Nabavi, S. Paredes, A.S.G. Khalil, B. Michel, D. Poulikakos, An experimentally optimized model for heat and mass transfer in direct contact membrane distillation, Int. J. Heat Mass Trans. 66 (2013) 855–867.

[24] S. Pazokifard, S.M. Mirabedini, M. Esfandeh, S. Farrokhpay, Fluoroalkylsilane treatment of TiO_2 nanoparticles in difference pH values: Characterization and mechanism, Adv. Powder Technol. 23 (2012) 428–436.

[25] S.A. Ibrahim, S. Sreekantan, Effect of pH on TiO_2 nanoparticles via sol gel method, Adv. Mater. Res. 173 (2010) 184–189.

[26] S. Pazokifard, S. Farrokhpay, M. Mirabedini, M. Esfandeh, Surface treatment of TiO_2 nanoparticles via sol-gel method: Effect of silane type on hydrophobicity of the nanoparticles, Prog. Org. Coating. 87 (2015) 36–44.